

Chemical diversity among A–B stars with low rotational velocities: non-LTE abundance analysis

L. Mashonkina¹ ,¹★ T. Ryabchikova,¹ S. Alexeeva,² T. Sitnova¹ and O. Zatsarinny³

¹*Institute of Astronomy of the Russian Academy of Sciences, Pyatnitskaya Street 48, 119017 Moscow, Russia*

²*CAS Key Laboratory of Optical Astronomy, National Astronomical Observatories, Beijing 100101, China*

³*Department of Physics and Astronomy, Drake University, Des Moines, IA 50311, USA*

Accepted 2020 September 28. Received 2020 September 25; in original form 2020 August 31

ABSTRACT

We present accurate element abundance patterns based on the non-local thermodynamic equilibrium (non-LTE, NLTE) line formation for 14 chemical elements from He to Nd for a sample of nine A9 to B3-type stars with well-determined atmospheric parameters and low rotational velocities. We constructed new model atom of Zr II–III and updated model atoms for Sr II and Ba II by implementing the photoionization cross-sections from calculations with the Dirac *B*-spline *R*-matrix method. The NLTE abundances of He to Fe in the stars HD 17081, HD 32115, HD 160762, and HD 209459 are found to be consistent with the solar abundances, and HD 73666 being a Blue Straggler does not reveal deviations from chemical composition of the Praesepe cluster. Three of these stars with an effective temperature of lower than 10 500 K have supersolar abundances of Sr, Zr, Ba, and Nd, and our results suggest the presence of a positive correlation between stellar effective temperature and abundance. For each star, enhancement of Ba is higher than that for any other heavy element. We propose that the solar Ba abundance is not representative of the galactic Ba abundance at modern epoch. The status of HD 145788 was not clarified: This star has solar abundances of C to Si and enhancements of Sr to Ba similar to that for superficially normal stars of similar temperature, while Ca, Ti, and Fe are overabundant. The NLTE abundances of Vega support its status of a mild λ Bootis star.

Key words: line: formation – stars: abundances – stars: atmospheres.

1 INTRODUCTION

The range of A to middle B spectral types is known by chemical anomalies of various kinds. There exist magnetic (Ap), non-magnetic metallic-line (Am), non-magnetic mercury–manganese (HgMn), helium-weak (He-weak), λ Bootis-type stars. Most probably, only the surface layers of chemically peculiar (CP) stars possess chemical anomalies and their origin is connected with stellar magnetic fields and/or atomic diffusion that results from the competitive action of gravitational settling and radiative accelerations (Michaud 1970, 1980). For better understanding the mechanisms of chemical peculiarity, accurate abundance determinations are required for many elements, from the lightest He to the rare-Earth elements (REE), in each of the groups of CP stars.

With all the uncertainties in theoretical spectrum modelling and analysis of observed spectra, the most reliable abundance results can be obtained for non-magnetic stars with low rotational velocities. As observations suggest (Preston 1974, and references therein) and the theory supports (Michaud 1982), slow rotation (the equatorial velocity below 120 km s^{−1}) favours the presence of chemical anomalies in hot (A–B-type) stars. Nevertheless, the A–B stars with close-to-solar element abundance pattern, which are referred to as superficially normal stars, exist, as shown by S. Adelman and his collaborators in their series of papers (Adelman et al. 2000, and references therein) and by the other researchers (Lemke 1990; Hill & Landstreet 1993; Varenne

& Monier 1999; Bikmaev et al. 2002; Fossati et al. 2009; Royer et al. 2014). In order to make definite conclusions about abundance differences between superficially normal stars and the Sun and between superficially normal and Am stars, appropriate treatment of spectral line formation is required. However, the majority of abundance studies of A- to late B-type stars are still made under the local thermodynamic equilibrium (LTE) assumption. Exceptions are related to either selected stars or selected chemical elements. For example, for the benchmark A0 V star Vega, its abundances were derived based on the non-local thermal equilibrium (non-LTE = NLTE) line formation by Gigas (1986, Fe), Gigas (1988, Mg and Ba), Sturenburg & Holweger (1991, C), Steenbock & Holweger (1992, Al), Takeda (1992, C and N), Przybilla et al. (2000, 2001a), Przybilla, Butler & Kudritzki (2001b, O, Mg, and C), and Przybilla & Butler (2001, N). N. Przybilla and his collaborators calculate the NLTE abundance patterns (He, C, N, O, Mg, S, Ti, and Fe) for the selected A to late B supergiants (Przybilla et al. 2006; Schiller & Przybilla 2008), the CP star HVS 7 (Przybilla et al. 2008), and the Am star HD 131399A (Przybilla, Aschenbrenner & Buder 2017). The NLTE abundances of C, N, and O in samples of A-type supergiants and bright giants were derived by Venn (1995, C and N), Takeda & Takada-Hidai (2000, C), and Lyubimkov et al. (2011, 2015) and Lyubimkov, Korotin & Lambert (2019). For a sample of A and Am stars, Belyakova, Mashonkina & Sakhbullin (1999) reported the NLTE abundances of Sr.

This paper aims to determine the NLTE abundance patterns in the range from He to Nd (for 14 elements) for a sample of nine A9 to B3 stars with low rotational velocities ($V \sin i \lesssim 25$ km s^{−1}). The sample includes superficially normal as well as Am and suspected

* E-mail: lima@inasan.ru

Table 1. Atmospheric parameters of the sample stars and characteristics of the observed spectra.

Star	T_{eff} (K)	$\log g$	[Fe/H]	ξ_t (km s ⁻¹)	Ref.	$v \sin i$ (km s ⁻¹)	Ref.	Instrument	Observed spectra Source	$\lambda/\Delta\lambda$
HD 32115	7250	4.20	0.00	2.3	B02	9	B02	ESPaDOaS	CAO	60 000
HD 73666 (40 Cnc)	9380	3.78	0.10	1.8	F07	10	F07	ESPaDOaS	F07	65 000
HD 172167 (Vega)	9550	3.95	−0.50	1.8	CK93	23.5	R14	FOCES	A. Korn	40 000
HD 72660	9700	4.10	0.40	1.8	S16	7	R14	HIDES	T07	100 000
								ESPaDOaS	V. Khalack	65 000
								STIS	GL16	110 000
HD 145788	9750	3.70	0.46	1.3	F09	13	R14	HARPS	F09	115 000
HD 48915 (Sirius)	9850	4.30	0.40	1.8	HL93	16	HL93	ESPaDOaS	CAO	65 000
								GHRS	W3496	25 000
HD 209459 (21 Peg)	10 400	3.55	0.00	0.5	F09	4	S81	ESPaDOaS	CAO	120 000
HD 17081 (π Cet)	12 800	3.75	0.00	1.0	F09	20	F09	ESPaDOaS	F09	65 000
HD 160762 (ι Her)	17 500	3.80	0.02	1.0	NP12	6	NP12	ESPaDOaS	CAO	65 000

Note. Ref. Source: B02 = Bikmaev et al. (2002), CK93 = Castelli & Kurucz (1993), F07, F09 = Fossati et al. (2007), Fossati et al. (2009), GL16 = Golriz & Landstreet (2016), HL93 = Hill & Landstreet (1993), NP12 = Nieva & Przybilla (2012), R14 = Royer et al. (2014), S81 = Sadakane (1981), S16 = Sitnova et al. (2016), T07 = Takeda et al. (2007, <http://pasj.asj.or.jp/v59/n1/590122/590122-frame.html>), W3496 = GO Proposal 3496 by G. Wahlgren, CAO (Common Archive Observation data base) = <http://www.cfht.hawaii.edu/Instruments/Spectroscopy/Espadons/>.

Am stars with well-determined atmospheric parameters and high-quality observed spectra available. Since 2013, our group develops and carefully tests the NLTE methods for spectroscopic analyses of A–B-type stars. The results are already published for O I (Sitnova, Mashonkina & Ryabchikova 2013), C I–II (Alexeeva, Ryabchikova & Mashonkina 2016), Ti I–II (Sitnova, Mashonkina & Ryabchikova 2016), Mg I–II (Alexeeva et al. 2018), Ca I–II (Sitnova, Mashonkina & Ryabchikova 2018), He I (Korotin & Ryabchikova 2018), Si I–II–III (Mashonkina 2020), and Ne I (Alexeeva et al. 2020). The work on Fe I–II is in progress (Sitnova, in preparation). In this study, we present new NLTE treatments and extend the NLTE abundance analyses to Na I, Sr II, Zr II–III, Ba II, and Nd II–III.

The paper is organized as follows: Stellar sample, spectral observations, and atmospheric parameters are described briefly in Section 2. Section 3 presents new model atom for Zr II–III, updates of the model atoms for Sr II and Ba II, methods of the NLTE calculations, and the obtained NLTE effects for Na I, Sr II, Ba II, Zr II–III, and Nd II–III. In Section 4, we determine abundances of O, Na, Sr, Zr, Ba, and Nd in the sample stars. Stellar element abundance patterns are discussed in Section 5. We summarize our conclusions in Section 6.

2 STELLAR SAMPLE, OBSERVATIONS, ATMOSPHERIC PARAMETERS

Our sample includes the four superficially normal stars: HD 32115 (A9 V), HD 209459 (21 Peg, B9.5 V), HD 17081 (π Cet, B7 IV), and HD 160762 (ι Her, B3 IV), the two Am stars: HD 48915 (Sirius, A1 V) and HD 72660 (A0 V), a mild λ Bootis-type star HD 172167 (Vega, A0 V), and the two stars: HD 73666 (40 Cnc, A1 V) and HD 145788 (A0 V), which stay separately from the others. The latter reveals an overall enhancement of metals, but was not classified as Am star (Fossati et al. 2009). HD 73666 is a member of the Praesepe cluster and known as a Blue Straggler. Though Fossati et al. (2007) find that HD 73666 reveals typical chemical abundances of the Praesepe cluster and refer to this star as a normal A-type star, its origin was connected, most probably, with the collisional mergers of two stars or two binary systems (Fossati et al. 2010) that can affect a chemical composition of the resulting object. The

three of our stars, namely π Cet, HD 32115, and HD 72660, are primary components of single line spectroscopic binaries (SB1), with negligible flux coming from the secondary star. Sirius is a primary component of an astrometric visual binary system. ι Her is a slowly pulsating B-type (SPB, the β Cephei type) star. Vega is a rapidly rotating star seen pole-on. Similarly to our previous studies, we assume that it is safe to analyse the stars ignoring the presence of their secondaries for the SB1s, pulsations for ι Her, and the non-spherical effects for Vega.

Characteristics of spectral observations are listed in Table 1. For the seven stars, we used spectra observed with a spectral resolving power of $R = \lambda/\Delta\lambda > 60\,000$ and a signal-to-noise ratio of $S/N > 200$, using the ESPaDOaS instrument of the Canada–France–Hawaii Telescope. For two of them, J. Landstreet kindly provided us with the ultraviolet (UV) spectra observed on the *Hubble Space Telescope* with the Goddard High Resolution Spectrograph (GHRS) for Sirius (Henderson et al. 1999) and the Space Telescope Imaging Spectrograph (STIS) for HD 72660 (Golriz & Landstreet 2016). HD 145788 was observed with the Échelle spectrograph HARPS (High Accuracy Radial velocity Planet Searcher) attached at the 3.6-m ESO La Silla telescope. For Vega, we used spectra observed by A. Korn with the spectrograph FOCES (fibre optics Cassegrain Echelle spectrograph) at the 2.2-m telescope of the Calar Alto Observatory and by Takeda, Kawanomoto & Ohishi (2007) with the High-Dispersion Echelle Spectrograph (HIDES) at the coude focus of the 188-cm reflector at the Okayama Astrophysical Observatory.

For consistency with our earlier studies, for each star we used exactly the same effective temperature (T_{eff}), surface gravity ($\log g$), metallicity ([Fe/H]), and microturbulent velocity (ξ_t). The data and its sources are listed in Table 1. We refer to the original papers and also Alexeeva et al. (2016, 2018) and Sitnova et al. (2016) for a description of the methods of atmospheric parameter determinations.

Classical plane-parallel and LTE model atmospheres were calculated with the code LLMODELS (Shulyak et al. 2004). For Sirius, its model atmosphere was taken from R. Kurucz website.¹

¹<http://kurucz.harvard.edu/stars/sirius/ap04t9850g43k0he05y.dat>

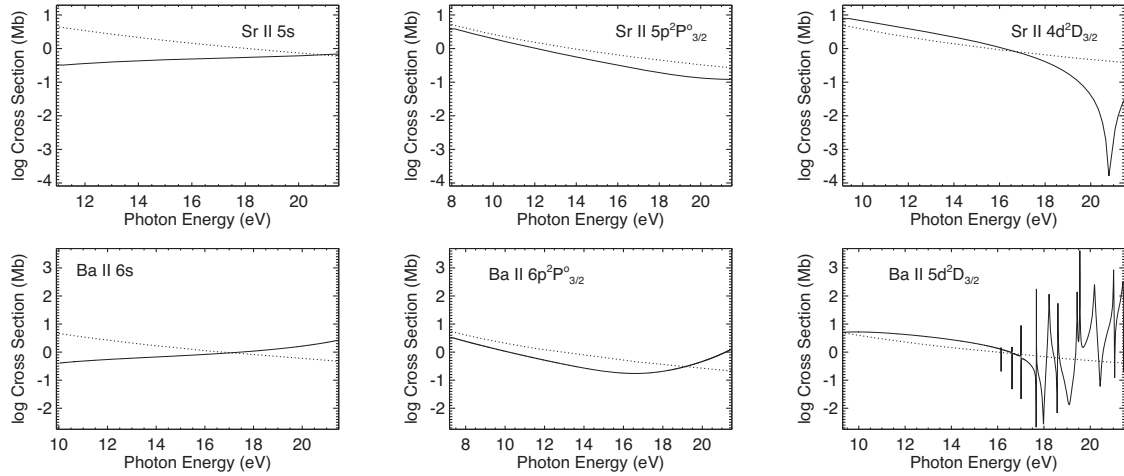


Figure 1. Photoionization cross-sections for the low-excitation levels of Sr II (top row) and Ba II (bottom row) as a function of photon energy from the calculations with the R-matrix method (solid curves) and in hydrogenic approximation (dotted curves).

3 NON-LTE CALCULATIONS

3.1 New model atom of Zr II–III

We produced a new model atom, which includes the model atom of Zr II, as constructed by Velichko, Mashonkina & Nilsson (2010), and the Zr III states with an excitation energy of $E_{\text{exc}} \lesssim 12.2$ eV (up to $5s5p\ ^1P^\circ$) from measurements of Reader & Acquista (1997), as provided by the National Institute of Standards and Technology (NIST) data base² (Kramida et al. 2019). The triplet fine structure was taken into account for the Zr III $4d^2\ ^3F$ and $4d^2\ ^3P$ terms. The Zr III levels above 12.2 eV were ignored because, in the stellar parameter range with which we concern, they do not affect the statistical equilibrium (SE) of zirconium and contribute less than 0.0001 per cent to the total abundance of Zr. Final model atom includes 247 levels of Zr II, 18 levels of Zr III, and the ground state of Zr IV.

Oscillator strengths predicted by R. Kurucz³ were used to compute radiative rates for 126 transitions of Zr III. We compared the adopted gf -values with predictions of Rynkun, Gaigalas & Jönsson (2020) for 112 transitions in common. Rynkun et al. (2020) provide slightly lower gf -values compared with that of R. Kurucz, by 0.06 ± 0.26 dex for all the transitions and by 0.09 ± 0.11 dex for 68 transitions with $\log gf > -1.5$. We note that Rynkun et al. (2020, see their fig. 5) underestimate the transition probabilities compared with laboratory measurements of Mayo, Ortiz & Campos (2005), by 0.07 dex, on average. Thus, our adopted gf -values agree very well the experimental data.

For both Zr II and Zr III, we did not find in the literature accurate data on photoionization and electron-impact excitation cross-sections. The photoionization cross-sections were calculated in the hydrogenic approximation, where a principal quantum number n was replaced with an effective principal quantum number n_{eff} . The formula of van Regemorter (1962) for allowed transitions and $\Upsilon = 1$ for forbidden transitions were applied to obtain the collisional rates. Ionization by electronic collisions was calculated from the Seaton (1962) formula, employing a hydrogenic photoionization cross-section at the threshold.

3.2 Update of the model atom for Sr II

A comprehensive model atom of Sr II was originally constructed by Belyakova & Mashonkina (1997) and updated in this study, as follows.

More Sr II energy levels, up to $n = 14$, with the data from NIST, were included in the atomic model. The doublet fine structure is taken into account for the Sr II $4d\ ^2D$ and $5p\ ^2P^\circ$ terms. Sr III is represented by the ground state because the excited states, with their excitation energies of $E_{\text{exc}} > 21.8$ eV, contribute only a little to the Sr abundance, even in the hot atmospheres. Oscillator strengths of the newly added transitions were taken from calculations of R. Kurucz.

In the atmospheres with $T_{\text{eff}} > 9000$ K, Sr II is strongly ionized, and its SE depends strongly on deviations of the mean intensity of ionizing radiation from the Planck function and the photoionization cross-sections. For the Sr II states from $5s$ to $8s$, the photoionization cross-sections were calculated in this study with the Dirac B -spline R -matrix (DBSR) method, in the same approximations as it was done for $h\nu + K I$ problem (Zatsarinny & Tayal 2010). New data for the three lowest terms are displayed in Fig. 1. The hydrogenic approximation (with n_{eff}) was used for the remaining levels in the model atom.

For all the transitions between $5s$ and up to $4f$, we apply electron-impact excitation rate coefficients from ab initio calculations of Bautista et al. (2002). The formula of van Regemorter (1962) for allowed transitions and the effective collision strength $\Upsilon = 1$ for forbidden transitions were used in the other cases. Ionization by electronic collisions was calculated as for Zr II–III.

3.3 Update of the model atom for Ba II

Similarly to Sr II, Ba II is a minority species in the atmospheres with $T_{\text{eff}} > 9000$ K. Therefore, the system of energy levels has to be fairly complete in the SE calculations. The model atom constructed by Mashonkina, Gehren & Bikmaev (1999) was extended by including all the Ba II levels up to $n = 50$, as provided by NIST (Kramida et al. 2019). The doublet fine structure was taken into account for the $5d\ ^2D$ and $6p\ ^2P^\circ$ terms. Only the ground state of Ba III was included because the excited states lie above $E_{\text{exc}} = 16.5$ eV and do not affect the SE of barium. For the transitions missing in model atom of Mashonkina et al. (1999), their radiative rates were computed with oscillator strengths predicted by R. Kurucz.

²<https://physics.nist.gov/PhysRefData/ASD>

³<http://kurucz.harvard.edu/atoms/>

Table 2. Line atomic data and LTE (L) and NLTE (N) abundances, $\log \varepsilon$, from individual lines in the sample stars.

Atom	E_{exc}	$\log gf$	$\log \Gamma_4/N_e$	$\log \Gamma_6/N_H$	HD 32115		...	HD 72660		...	21 Peg	...	ι Her		
					L	N	...	L	N	...	L	N	...	L	N
O I															
7771.94	9.15	0.37	−5.55	−7.47	9.69	9.01	...	9.65	8.49	...	10.14	8.60	...	10.35	8.68
Na I															
5682.63	2.10	−0.71	−3.88	−6.86	6.18	6.11	...	6.74	6.64	...	−	−	...	−	−
8194.82	2.10	0.49	−4.97	−7.23	6.76	6.23	...	−	−	...	6.52	6.23	...	−	−
8194.79	2.10	−0.46	−4.97	−7.23	−	−	...	−	−	...	−	−	...	−	−
Sr II															
4077.71	0.0	0.15	−6.22	−7.71	3.30	3.37	...	4.24	4.38	...	2.89	3.48	...	−	−
Ba II															
4554.03	0.0	0.17	−5.31	−7.73	2.78	2.69	...	3.58	3.68	...	2.75	3.13	...	−	−

Notes. Γ_4/N_e and Γ_6/N_H in $\text{rad s}^{-1} \text{cm}^3$. This table is available in its entirety in a machine-readable form in the online journal. A portion is shown here for guidance regarding its form and content.

The photoionization cross-sections for the Ba II states from 6s to 6f were calculated in this study with the DBSR method, following Zatsarinny & Tayal (2010). Fig. 1 displays new data for the three lowest terms. For the remaining levels in the model atom, we applied the hydrogenic approximation with n_{eff} .

Experimental data of Crandall, Taylor & Dunn (1974) are available for electron-impact excitation of the Ba II 6p, 7s, and 6d levels from the ground state. For all the remaining transitions between 6s and 6d, we applied the collision cross-sections computed by Sobelman, Vainshtein & Yukov (1981) in the Born approximation. If the data are absent, the formula of van Regemorter (1962) for allowed transitions and $\Upsilon = 1$ for forbidden transitions have been adopted. Ionization by electronic collisions was calculated as for Zr II–III.

3.4 Oxygen, sodium, neodymium

The O I model atom of Przybilla et al. (2000) and Sitnova et al. (2013) was updated, by calculating radiative rates of strong UV bound–bound (b–b) transitions with the Voigt absorption profiles. With this model atom, we revised the NLTE abundances of oxygen in HD 32115, Vega, and Sirius compared with those of Sitnova et al. (2013) and determined the O abundances of the remaining stellar sample.

Non-LTE calculations for Na I were performed with the model atom of Alexeeva, Pakhomov & Mashonkina (2014) and for Nd II–III, using the model atom of Mashonkina, Ryabchikova & Ryabtsev (2005).

3.5 Codes, list of investigated lines

All the NLTE species were treated as the trace ones assuming that atmospheric structure is not affected by deviations of their level populations from the thermodynamic equilibrium ones and the SE calculations can be performed with fixed LTE model atmosphere. Przybilla, Nieva & Butler (2011) showed that such a hybrid method is able to reproduce observations for $T_{\text{eff}} = 15\,000$ to $35\,000$ K. This is all the more true for our cooler atmospheres. We employed a modified version of the DETAIL code (Butler & Giddings 1985; Przybilla et al. 2011) to solve the coupled radiative transfer and SE equations.

Spectral lines used in abundance analyses, together with their atomic parameters, are listed in Table 2.

In the visual and near-infrared (IR) spectral range of most of our stars with $T_{\text{eff}} \leq 10\,400$ K, sodium and barium are well represented, by up to eight lines of Na I and five lines of Ba II, while strontium, zirconium, and neodymium are observed in two lines, at most. The exception is HD 72660, for which we measured six lines of Zr III

in the UV spectrum. For lines of Na I and Sr II, we used gf -values recommended by NIST. Laboratory gf -values from De Munshi et al. (2015) and Dutta et al. (2016) were adopted for lines of Ba II and from Ljung et al. (2006) for Zr II. For Zr III and Nd III, gf -values are provided by the Vienna Atomic Line Database (VALD; Ryabchikova et al. 2015). Hyperfine splitting (HFS) and/or isotopic components were taken into account for lines of Ba II and Sr II, using the data from McWilliam (1998) and Borghs et al. (1983), respectively. The fractional isotope abundances correspond to the Solar system matter (Lodders, Plame & Gail 2009).

For lines of Na I and Ba II, quadratic Stark effect broadening was treated using the full width at half-maximum intensity from the STARK-B⁴ data base. For the Sr II resonance lines, $\log \Gamma_4 = -5.40$ was computed by E. Yukov, as published by Khokhlova & Riabchikova (1975). For the remaining lines, the Γ_4 values were computed from the approximate formula of Cowley (1971). Van der Waals broadening is important only for the coolest star of our sample, HD 32115. We applied accurate Γ_6 values from Barklem, Piskunov & O’Mara (2000) for lines Na I, Sr II, and Ba II. For the remaining lines, van der Waals broadening was taken into account with the Unsold (1955) formula.

We also included the Sc II lines in our analysis because the Sc abundance is often used as one of the characteristics in Am-star classification. Abundances of Sc were determined under the LTE assumption. Expected NLTE effects are discussed in Section 4.3. Laboratory gf -values of the Sc II lines were taken from Lawler & Dakin (1989) and the HFS components were calculated by Pakhomov, Ryabchikova & Piskunov (2019) using experimental data of Mansour et al. (1989) and Villemoes et al. (1992).

Abundances from individual lines were derived from line profile fitting, but not from equivalent widths (EWs). Exceptions are Vega, where the line profiles have a rectangular shape, and the LTE abundances from the O I 7771, 7774, 7775 Å lines, whose profiles in each star cannot be reproduced under the LTE assumption. In order to compute the synthetic spectra, we used the SYNTHV_NLTE code (Tsymbal, Ryabchikova & Sitnova 2019), which implements the pre-computed departure coefficients from DETAIL. The line list required for calculations of the synthetic spectra, together with atomic data, was taken from VALD. The IDL BINMAG code by O. Kochukhov⁵ was used to obtain the best fit to the observed spectrum. An EW analysis was made also with the SYNTHV_NLTE + IDL BINMAG code.

⁴<https://stark-b.obspm.fr>

⁵<http://www.astro.uu.se/~oleg/binmag.html>

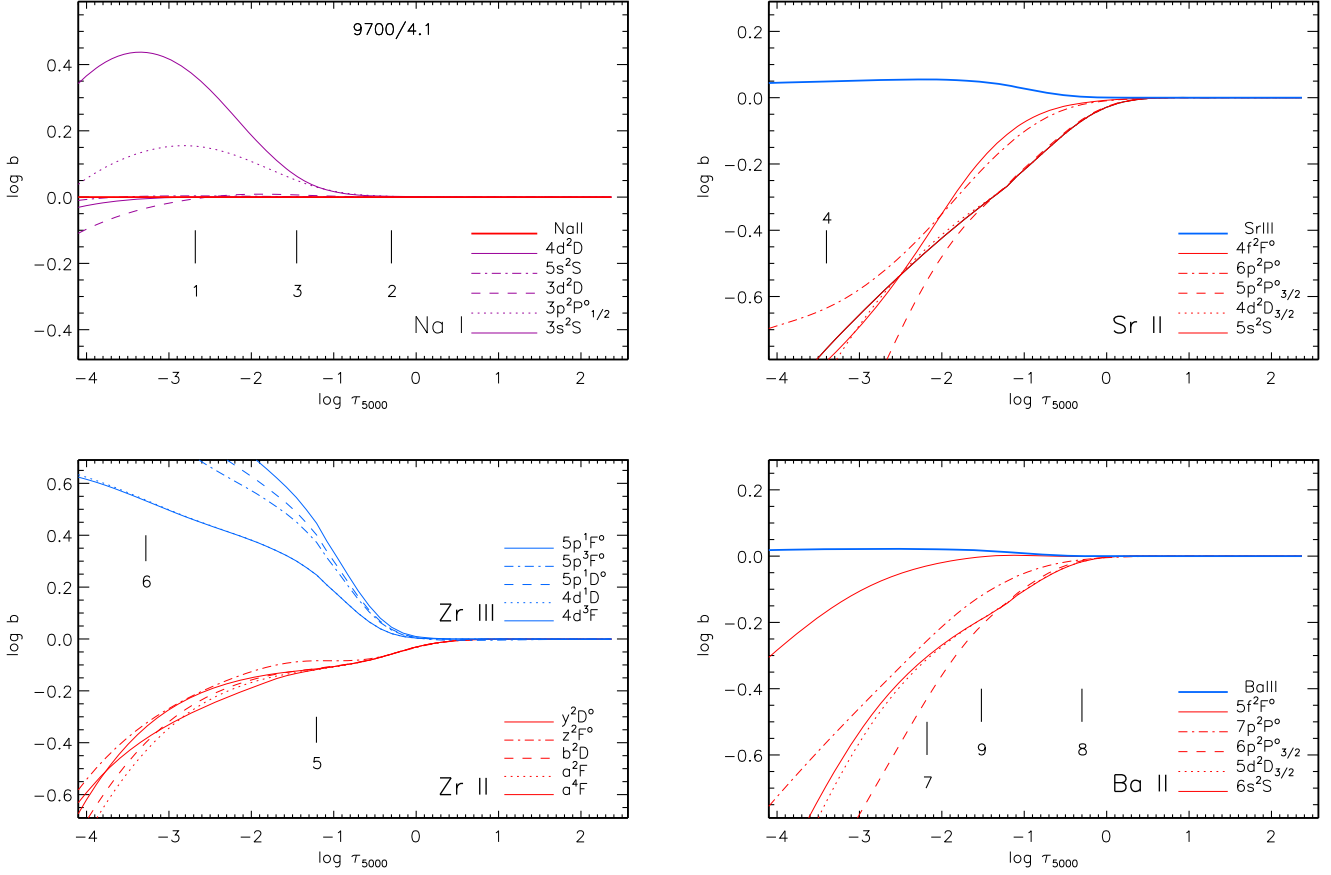


Figure 2. Departure coefficients, b , for the levels of Na I (top left panel), Sr II (top right panel), Zr II–Zr III (bottom left panel), and Ba II (bottom right panel) as a function of $\log \tau_{5000}$ in the model atmosphere 9700/4.10/0.4. The selected levels are quoted in the right part of each panel. Tick marks indicate the locations of line centre optical depth unity for the following lines: Na I 5889 (1), 5688 (2), and 8194 Å (3), Sr II 4077 Å (4), Zr II 4149 Å (5), Zr III 1790 Å (6), and Ba II 4554 (7), 5853 (8), and 6141 Å (9).

3.6 Non-LTE effects

The NLTE effects for C I–II, O I, Ne I, Mg I–II, Si I–II–III, Ca I–II, and Ti I–II were discussed in detail in our previous papers. Here, we concentrate on the new NLTE species. For each of them, a behaviour of the departure coefficients, $b = n_{\text{NLTE}}/n_{\text{LTE}}$, is similar in the model atmospheres with $T_{\text{eff}} > 9000$ K. Here, n_{NLTE} and n_{LTE} are the SE and thermal (Saha–Boltzmann) number densities, respectively. We select the model with $T_{\text{eff}}/\log g/[\text{Fe}/\text{H}] = 9700/4.10/0.4$ to display $\log b$ for the selected levels of Na I, Sr II, Zr II–Zr III, and Ba II in Fig. 2.

3.6.1 Na I

NLTE leads to an overpopulation of the Na I ground ($3s$) and first excited ($3p$) levels due to the cascade from upper levels induced by the escape of line photons (photon-suction effect, as called by Bruls, Rutten & Shchukina 1992). Lines of Na I are strengthened, and the NLTE abundance corrections, $\Delta_{\text{NLTE}} = \log \varepsilon_{\text{NLTE}} - \log \varepsilon_{\text{LTE}}$, are negative. The NLTE effects are stronger for the 5889 and 5895 Å resonance lines compared with the subordinate lines, and, for the subordinate lines arising from common $3p$ level, they are stronger for the stronger lines, which form in the higher atmospheric layers. For example, in the 9700/4.10/0.4 model, $\Delta_{\text{NLTE}} = -0.77$, -0.47 , and -0.10 dex for Na I 5889, 8194, and 5688 Å, respectively. Magnitude of Δ_{NLTE} depends weakly on T_{eff} .

3.6.2 Sr II and Ba II

For both species, the NLTE mechanism depends on T_{eff} . In the atmosphere of our coolest star, HD 32115, Sr II and Ba II are the majority species, and the NLTE effects are mostly determined by dropping the line source function (S_{ν}) below the Planck function (B_{ν}) in the line formation layers. Lines of Sr II and Ba II are strengthened, and the NLTE abundance corrections are negative, with $\Delta_{\text{NLTE}} = -0.04$, -0.09 , and -0.21 dex for Sr II 4077 Å, Ba II 4554, and 6496 Å, respectively.

In hot atmospheres, with $T_{\text{eff}} > 9000$ K, Sr II and Ba II are strongly ionized, and the main NLTE mechanism is the overionization caused by superthermal radiation of a non-local origin below the thresholds of the $4d$ and $5p$ levels for Sr II and the $5d$ and $6p$ levels for Ba II. A depletion of the level populations in the line formation layers (Fig. 2) results in weakened lines and positive NLTE abundance corrections, which grow towards higher T_{eff} . For example, $\Delta_{\text{NLTE}} = 0.35$ and 0.26 dex for Sr II 4077 Å and Ba II 4554 Å, respectively, in the 9380/3.78/0.10 model, and the corresponding numbers are 0.59 and 0.38 dex in the 10400/3.55/0.0 model.

3.6.3 Zr II–III

Similarly to Sr II and Ba II, Zr II moves from a majority species in the 7250/4.20/0.0 model to a minority one for $T_{\text{eff}} > 9000$ K. However, Zr II has a different atomic term structure compared with that of Sr II

and Ba II, such that NLTE leads to slightly weakened lines of Zr II in our coolest model atmosphere, with $\Delta_{\text{NLTE}} = 0.05\text{--}0.08$ dex for different lines. For $T_{\text{eff}} > 9000$ K, Zr II is subject to overionization and Δ_{NLTE} grows towards higher T_{eff} . For example, for Zr II 4149 Å, $\Delta_{\text{NLTE}} = 0.19$ and 0.51 dex in the 9380/3.78/0.10 and 10400/3.55/0.0 models, respectively.

Thanks to relatively high ionization energy of Zr II ($\chi_{\text{ion}} \simeq 13.1$ eV), Zr III and Zr II have comparable number densities in the atmospheres with $T_{\text{eff}} = 9700$ and 9850 K. Therefore, overionization of Zr II in the line formation layers leads to enhanced populations of the Zr III levels (Fig. 2) and strengthened lines of Zr III, with negative NLTE abundance corrections. In the 9700/4.10/0.40 model, $\Delta_{\text{NLTE}} = (-0.10)\text{--}(-0.17)$ dex for different lines.

3.6.4 Nd II–III

Lines of Nd II were measured only in our coolest star, HD 32115. In its atmosphere, Nd II is a majority species and NLTE leads to slightly weakened lines, with $\Delta_{\text{NLTE}} = 0.12$ dex for both Nd II 4706 and 5319 Å.

Nd III is a majority species in the atmospheres with $T_{\text{eff}} > 9000$ K. The NLTE effects are minor, with $\Delta_{\text{NLTE}} \leq 0.01$ dex in absolute value for the lines at 5294 and 5203 Å, which arise from the ground term.

3.7 Comparison with other NLTE studies

In the stellar parameter range, with which we concern, the NLTE calculations for Na I were performed by Takeda et al. (2009). For Na I 5889 and 5895 Å in Sirius, with slightly higher $T_{\text{eff}} = 9938$ K compared with ours, by 90 K, Takeda et al. (2009) report the average $\Delta_{\text{NLTE}} = -0.67$ dex. We could not measure Na I 5889 Å in Sirius and obtained $\Delta_{\text{NLTE}} = -0.56$ dex for the second resonance line. We note that, in all the cases where both lines were measured, we calculated greater Δ_{NLTE} for Na I 5889 Å compared with that for Na I 5895 Å. For example, $\Delta_{\text{NLTE}} = -0.77$ and -0.54 dex for Na I 5889 and 5895 Å, respectively, in the 9700/4.10/0.40 model.

Gigas (1988) perform the NLTE calculations for Ba II in Vega and report $\Delta_{\text{NLTE}} = 0.30$ and 0.27 dex for Ba II 4554 and 4934 Å, respectively. We obtain larger NLTE abundance corrections, by 0.09 and 0.10 dex.

4 ABUNDANCE RESULTS

The LTE and NLTE abundances from individual lines of O I, Na I, Sr II, Zr II–III, Ba II, and Nd II–III, as well as the LTE abundances from lines of Sc II, are presented in Table 2 for each star. We use the abundance scale where $\log \varepsilon_{\text{H}} = 12$. Tables 3 and 4 present average LTE and NLTE abundances of the chemical elements studied in this paper, as well as of He, C, Ne, Mg, Si, Ca, and Ti from our previous papers (Alexeeva et al. 2016, 2018, 2020; Sitnova et al. 2016, 2018; Korotin & Ryabchikova 2018; Mashonkina 2020, respectively). Abundances of C and Mg in HD 32115 and HD 145788, which are missing in the papers of Alexeeva et al. (2016, 2018), and abundance of Ti in Vega, which is missing in Sitnova et al. (2016), were derived in this study. Errors of the average abundances were calculated as the dispersions in the single line measurements around the mean: $\sigma_1 = \sqrt{\sum (\bar{x} - x_i)^2 / (N_1 - 1)}$. Here, N_1 is the total number of used lines. In case of $N_1 = 1$, $\sigma_1 = 0.1$ dex was adopted. In order to compute the $[X/H]$ values, we employ the Solar system abundances of Lodders et al. (2009).

Detailed NLTE analysis of Fe I–II is in progress (Sitnova, in preparation), and we provide here preliminary average abundances. The Fe III-based LTE abundance of ι Her was calculated using 21 lines from the list of Nieva & Przybilla (2012). Our average LTE abundance is lower than the NLTE abundance of NP12, by 0.14 dex.

Figs 3, 4, and 5 display the LTE and NLTE abundances $[X/H]$ for different chemical species in the individual stars.

4.1 Oxygen

We preferred to use a common line list for all the sample stars and selected the two triplets, O I 6155, 6156, 6158 Å and O I 7771, 7774, 7775 Å. For HD 145788, only the first triplet was used because the IR lines are not covered by the observed spectrum.

The NLTE abundance corrections are negative for the O I lines and grow, in absolute value, towards higher T_{eff} . However, in any given star, a magnitude of Δ_{NLTE} is rather different for the visual and the IR lines. For example, $\Delta_{\text{NLTE}}(\text{O I } 6155 \text{ Å})$ varies between -0.03 dex (HD 32115) and -0.22 dex (ι Her), while $\Delta_{\text{NLTE}}(\text{O I } 7771 \text{ Å})$ varies between -0.68 and -1.67 dex. For each star, NLTE leads to consistent abundances from different lines, with an abundance spread of no more than 0.17 dex (HD 32115), while the difference in LTE abundances reaches 1.3 dex (π Cet).

4.2 Sodium

The Na I 5889, 5895 Å resonance lines are observed in a broad temperature range, up to $T_{\text{eff}} = 12\,800$ K. However, the stellar lines can be blended by the interstellar medium (ISM) and/or telluric lines. This is clearly the case in Vega and HD 145788. In the same stars, we could not measure also Na I 5682, 5688 Å due to affecting by the telluric lines.

Abundances derived from the resonance lines appear higher compared with that from the subordinate lines, even in the stars without signatures of the ISM absorption. NLTE reduces the abundance difference (resonance – subordinate), but does not cancel it completely, leaving 0.09 dex (Sirius) to 0.30 dex (21 Peg). Only for π Cet, the NLTE abundances from Na I 5889, 5895 Å and Na I 8194 Å are consistent, within 0.05 dex. In their NLTE analysis of about 120 A-type main-sequence stars, Takeda et al. (2009) conclude that the Na I resonance lines cannot be used as a reliable abundance indicator. We support this conclusion and do not account for the resonance lines in the average abundances. The exception is π Cet.

In five stars, we could measure the IR lines at 8183 and/or 8194 Å. NLTE leads to fairly consistent abundances from different subordinate lines, while the difference in LTE abundances between Na I 8183, 8194 Å and Na I 5682, 5688 Å amounts to 0.16 dex (21 Peg) to 0.5 dex (HD 32115).

4.3 Scandium

The NLTE calculations for Sc II were only performed in the literature for late-type stars (Zhang, Gehren & Zhao 2008; Zhao et al. 2016) and resulted in slightly positive NLTE abundance corrections. The ionization energy of Sc II is $\chi_{\text{ion}} \simeq 12.8$ eV. For $T_{\text{eff}} > 9000$ K, Sc II is effectively ionized in the atmosphere and is expected to be subject to overionization, similarly to that for Zr II, which has close $\chi_{\text{ion}} \simeq 13.1$ eV. The NLTE abundance corrections computed for lines of Zr II

Table 3. Mean LTE (L) and NLTE (N) abundances, $\log \epsilon$, for the sample stars.

Atom		HD 32115	HD 73666	Vega	HD 72660	HD 145788	Sirius	21 Peg	π Cet
He ^a	N	–	10.94(0.03)	10.99(0.04)	10.72(0.04)	–	10.82(0.03)	10.90(0.02)	10.94(0.01)
	[He/H]	–	0.01	0.06	–0.21	–	–0.11	–0.03	0.01
C	L	8.55(0.22)	8.62(0.16)	8.65(0.28)	8.00(0.12)	8.37(0.08)	7.73(0.14)	8.36(0.23)	8.41(0.11)
	N	8.45(0.08)	8.57(0.08)	8.34(0.13)	8.02(0.08)	8.32(0.07)	7.71(0.14)	8.38(0.09)	8.45(0.09)
O	[C/H]	0.06(9)	0.18(19)	–0.05(19)	–0.37(6)	–0.07(5)	–0.69(14)	–0.01(25)	0.06(9)
	L	9.35(0.36)	9.82(0.41)	9.65(0.36)	9.30(0.43)	8.90(0.06)	9.17(0.41)	9.85(0.43)	9.94(0.44)
O	N	8.86(0.11)	8.90(0.08)	8.60(0.05)	8.43(0.07)	8.75(0.02)	8.44(0.05)	8.63(0.02)	8.72(0.02)
	[O/H]	0.13(6)	0.17(6)	–0.13(6)	–0.30(6)	0.02(3)	–0.29(5)	–0.10(6)	–0.01(6)
Ne	L	–	–	–	–	–	–	8.16(0.04)	8.35(0.07)
	N	–	–	–	–	–	–	8.00(0.05)	8.07(0.06)
Ne	[Ne/H]	–	–	–	–	–	–	–0.05(0)	0.02(15)
Na	L	6.47(0.38)	6.76(0.20)	–	6.76(0.02)	–	6.80(0.15)	6.45(0.11)	6.71(0.06)
	N	6.17(0.07)	6.47(0.01)	–	6.66(0.02)	–	6.54(0.02)	6.24(0.01)	6.37(0.05)
Mg	[Na/H]	–0.12(6)	0.18(4)	–	0.37(2)	–	0.25(3)	–0.05(2)	0.08(3)
	L	7.61(0.08)	7.87(0.17)	7.09(0.07)	7.92(0.16)	7.78(0.18)	7.66(0.18)	7.61(0.15)	7.62(0.11)
Mg	N	7.58(0.06)	7.70(0.04)	7.05(0.04)	7.77(0.06)	7.57(0.07)	7.51(0.06)	7.50(0.04)	7.57(0.05)
	[Mg/H]	0.04(12)	0.16(22)	–0.49(12)	0.23(21)	0.03(10)	–0.03(17)	–0.04(21)	0.03(16)
Si	L	7.66(0.18)	7.81(0.25)	7.08(0.17)	7.86(0.20)	7.90(0.19)	7.84(0.18)	7.60(0.28)	7.62(0.24)
	N	7.59(0.15)	7.67(0.16)	6.92(0.15)	7.83(0.09)	7.60(0.12)	7.72(0.11)	7.50(0.13)	7.75(0.13)
Ca	[Si/H]	0.06(20)	0.14(14)	–0.61(8)	0.30(20)	0.07(7)	0.19(11)	–0.03(18)	0.22(21)
	L	6.53(0.29)	6.47(0.13)	5.82(0.10)	6.58(0.11)	6.43(0.10)	5.88(0.08)	5.95(0.17)	5.91(0.59)
Ca	N	6.39(0.09)	6.52(0.05)	6.03(0.10)	6.62(0.09)	6.75(0.07)	6.09(0.05)	6.30(0.15)	6.40(0.00)
	[Ca/H]	0.08(36)	0.21(21)	–0.28(10)	0.31(31)	0.44(13)	–0.22(12)	–0.01(7)	0.09(3)
Sc	L	3.22(0.10)	3.02(0.02)	–	2.63(0.05)	3.05(0.04)	1.99(0.11)	2.60(0.05)	2.61(0.10)
	[Sc/H]	0.15(8)	–0.05(6)	–	–0.43(6)	–0.02(6)	–1.08(4)	–0.47(6)	–0.46(1)
Ti	L	4.73(0.06)	5.27(0.17)	4.50(0.02)	5.49(0.11)	5.28(0.15)	5.20(0.06)	4.80(0.05)	4.63(0.09)
	N	4.76(0.05)	5.19(0.08)	4.50(0.02)	5.45(0.08)	5.23(0.07)	5.15(0.04)	4.80(0.04)	4.90(0.08)
Fe ^b	[Ti/H]	–0.17(15)	0.26(8)	–0.43(6)	0.52(41)	0.30(32)	0.22(6)	–0.13(46)	–0.03(11)
	L	7.56(0.11)	7.70(0.10)	7.06(0.30)	8.08(0.16)	7.79(0.10)	7.99(0.06)	7.53(0.07)	7.39(0.08)
Fe ^b	N	7.55(0.11)	7.70(0.10)	7.05(0.17)	8.10(0.16)	7.76(0.07)	7.98(0.06)	7.51(0.07)	7.38(0.10)
	[Fe/H]	0.09	0.24	–0.41	0.67	0.30	0.52	0.05	–0.08
Sr	L	3.33(0.04)	3.00(0.04)	2.03(0.01)	4.20(0.06)	3.37(0.04)	3.53(0.00)	2.89(0.00)	2.64(0.10)
	N	3.28(0.04)	3.38(0.00)	2.71(0.01)	4.35(0.04)	3.28(0.01)	3.83(0.04)	3.49(0.01)	2.97(0.10)
Zr	[Sr/H]	0.38(2)	0.48(2)	–0.19(2)	1.45(2)	0.38(2)	0.93(2)	0.59(2)	0.07(1)
	L	2.75(0.04)	2.82(0.01)	2.17(0.10)	3.92(0.17)	2.87(0.11)	3.39(0.13)	2.41(0.10)	–
Ba	N	2.82(0.03)	3.01(0.00)	2.42(0.10)	3.85(0.11)	2.93(0.09)	3.40(0.13)	2.92(0.10)	–
	[Zr/H]	0.25(3)	0.44(2)	–0.15(1)	1.28(8)	0.36(2)	0.84(2)	0.35(1)	–
Ba	L	2.64(0.17)	2.86(0.05)	1.70(0.04)	3.54(0.03)	2.90(0.07)	3.58(0.06)	2.78(0.05)	–
	N	2.47(0.07)	3.11(0.04)	2.14(0.02)	3.67(0.03)	2.90(0.05)	3.74(0.06)	3.16(0.05)	–
Nd	[Ba/H]	0.29(3)	0.93(5)	–0.04(3)	1.49(5)	0.72(3)	1.56(5)	0.98(3)	–
	L	1.31(0.01)	1.94(0.03)	–	2.74(0.04)	–	2.94(0.03)	1.96(0.00)	–
Nd	N	1.43(0.01)	1.94(0.03)	–	2.73(0.04)	–	2.93(0.03)	1.95(0.01)	–
	[Nd/H]	–0.04(2)	0.47(2)	–	1.26(2)	–	1.46(2)	0.48(2)	–

Notes. ^aFrom Korotin & Ryabchikova (2018), ^bSitnova (in preparation). The numbers in parentheses are the dispersions in the single line measurements around the mean and the numbers of used lines.

Table 4. LTE and NLTE abundances, $\log \epsilon$, of ι Her.

Species	LTE	NLTE	n_l	[X/H]
He I ^a	–	10.91(0.02)	–	–0.02
C II	8.58(0.26)	8.43(0.10)	14	0.04
O I	9.94(0.46)	8.70(0.02)	3	–0.03
Ne I	8.65(0.14)	8.04(0.04)	18	–0.01
Mg II	7.61(0.14)	7.55(0.07)	9	0.01
Si III	7.79(0.05)	7.54(0.07)	4	0.01
Ca II	6.78(0.10)	6.59(0.10)	1	0.28
Fe II ^b	7.26(0.04)	7.40(0.03)	6	–0.06
Fe III	7.46(0.06)	–	21	0.00

Notes. ^aFrom Korotin & Ryabchikova (2018).

^bSitnova (in preparation).

can be used to get an idea of magnitudes of the NLTE abundance corrections for lines of Sc II.

4.4 Strontium

Only the Sr II 4077 and 4215 Å resonance lines were measured in spectra of our eight stars. In the hottest star, ι Her, these lines cannot be extracted from noise. In HD 32115, the lines are very strong, with $EW > 260$ mÅ, and probably cannot be reliable abundance indicators.

4.5 Zirconium

For our seven stars with $T_{\text{eff}} \leq 10\,400$ K, we could use one to three lines of Zr II in the visible spectral range. Six nearly clean lines of Zr III were found in the UV spectrum of HD 72660 and the

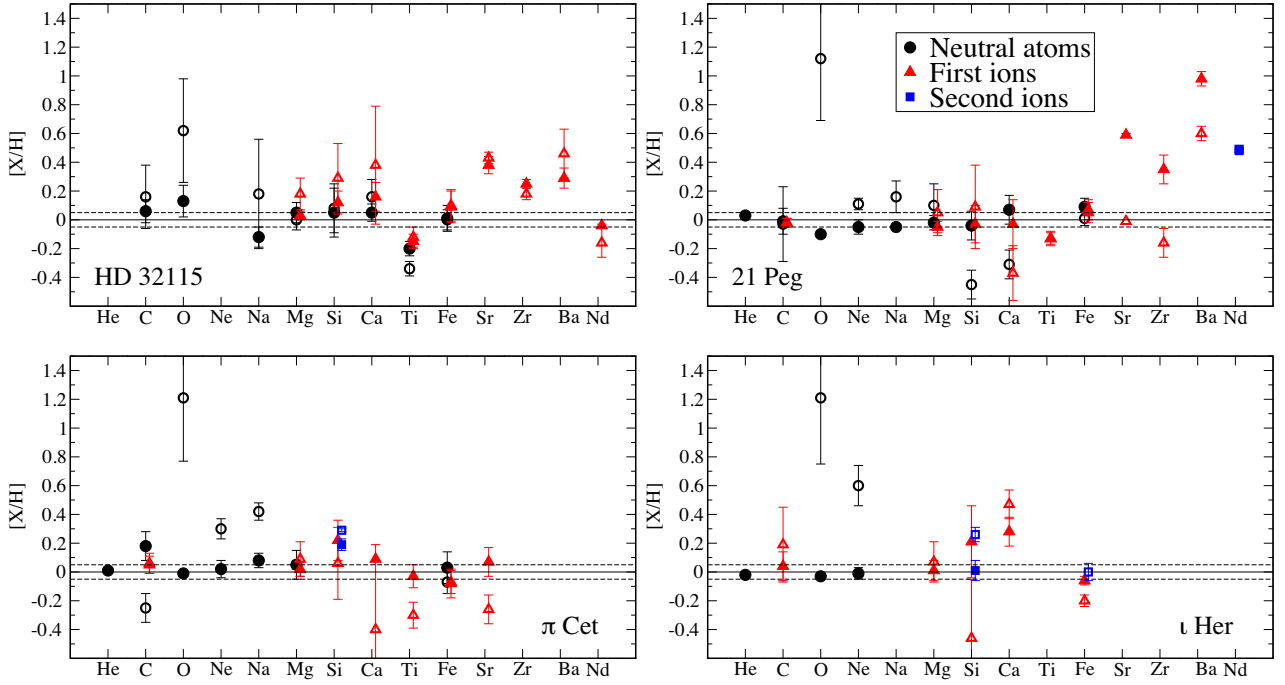


Figure 3. NLTE (filled symbols) and LTE (open symbols) $[X/H]$ abundances from lines of neutral atoms (circles), first ions (triangles), and second ions (squares) in HD 32115, 21 Peg, π Cet, and ι Her. The short-dashed lines indicate a typical uncertainty of 0.05 dex in the Solar system abundances of Lodders et al. (2009).

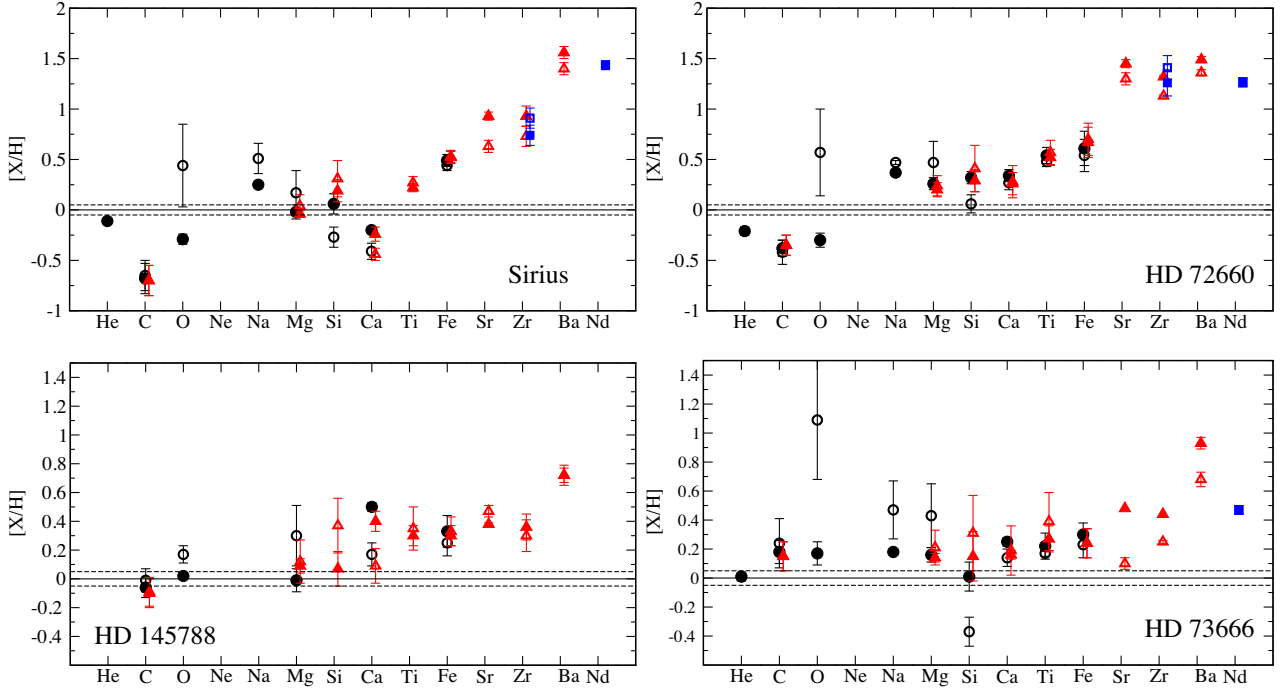


Figure 4. The same as in Fig. 3 for Sirius, HD 72660, HD 145788, and HD 73666.

only suitable line of Zr III, at 1790 Å, in Sirius. For HD 72660, NLTE leads to fairly consistent abundances from the two ionization stages, while the difference in LTE abundances amounts to $\log \epsilon(\text{Zr II} - \text{Zr III}) = -0.28$ dex. Using one line of Zr II and one line of Zr III in Sirius, we obtain a discrepancy between the two ionization stages, which, in LTE and NLTE, is very similar in absolute value, but of opposite sign, of -0.18 and 0.19 dex, respectively.

4.6 Barium

In each star with $T_{\text{eff}} \leq 10\,400$ K, we measured the Ba II 4554 and 4934 Å resonance lines and one to three lines of the Ba II 5d – 6p triplet. In HD 32115, the resonance lines are very strong, with $\text{EW} \simeq 200$ mÅ, and probably cannot be reliable abundance indicators. We obtained an abundance discrepancy between the resonance and subordinate lines of 0.18 and 0.22 dex, in LTE and NLTE, respectively, and excluded Ba II 4554 and 4934 Å from calculating the

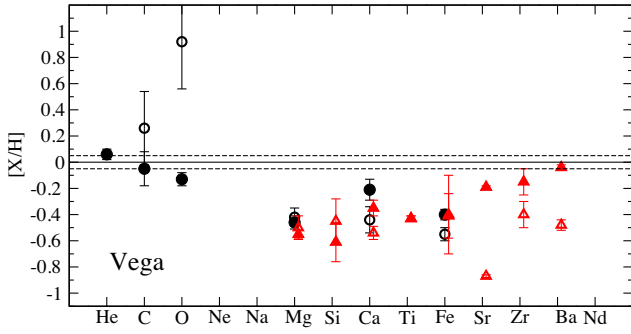


Figure 5. The same as in Fig. 3 for Vega.

Ba mean abundance of HD 32115. In contrast, consistent abundances from the resonance and subordinate lines were found in the remaining six stars, with an abundance difference of (0.02)–(−0.12) dex in different stars.

4.7 Neodimium

We could derive the Nd abundance for five stars of our sample. Two lines of Nd II were measured in the coolest star, HD 32115, and two lines of Nd III in each of the four stars, which reveal enhancements of the heavy elements beyond the iron group.

5 DISCUSSION

In this section, we discuss common features and distinctions in element abundance patterns of our sample stars, which belong to the groups of superficially normal, Am, and λ Bootis-type stars. We inspect carefully an element abundance pattern of our Blue Straggler star and attempt to understand the nature of HD 145788, with an unidentified type of chemical peculiarity.

5.1 Superficially normal stars

For each of our four superficially normal stars, the NLTE abundances of the elements in the range from He to Fe were found to be consistent with the solar values of Lodders et al. (2009), within 0.1 dex, as seen from Fig. 3. There are following three exceptions. (i) Titanium is subsolar in HD 32115, independent of NLTE or LTE, with $[\text{Ti}/\text{H}] = -0.17 \pm 0.05$ from the NLTE calculations of 15 lines of Ti I and Ti II. (ii) Silicon is supersolar in π Cet, with $[\text{Si}/\text{H}] = 0.22 \pm 0.13$ in NLTE (21 lines of Si II and Si III). LTE leads to the lower Si enhancement, but substantially larger line-to-line scatter: $[\text{Si}/\text{H}] = 0.09 \pm 0.24$. (iii) The only calcium absorption line, Ca II 3933 Å, was measured in ι Her, and it suggests an enhancement of calcium, with $[\text{Ca}/\text{H}] = 0.28$ in NLTE and even larger value in LTE, by 0.19 dex.

We stress that not only absorption, but also emission lines of C I (21 Peg, π Cet, ι Her), Si II (ι Her), and Ca II (ι Her) were well reproduced in our NLTE calculations with classical plane-parallel model atmospheres (Alexeeva et al. 2016; Sitnova et al. 2018; Mashonkina 2020) providing one more evidence for a status of these stars as normal stars.

The elements beyond Fe are worth to be discussed separately. Each of the four elements Sr, Zr, Ba, and Nd in 21 Peg is enhanced relative to its solar abundance, by more than 0.3 dex. In HD 32115, Zr and Ba are also supersolar, although to a less extent, with $[\text{Zr}/\text{H}] = 0.25$ and $[\text{Ba}/\text{H}] = 0.29$ dex, while $[\text{Nd}/\text{H}]$ is close to the solar value. The Sr II 4077 and 4215 Å lines in HD 32115 suggest overabundance of

Table 5. Changes in the NLTE abundances (Δ , dex) of Sr, Zr, Ba, and Nd in 21 Peg caused by variations in atmospheric parameters and atomic data.

		Sr	Zr	Ba	Nd
Atmospheric parameters:					
T_{eff} , −200 K	ΔT_{eff}	−0.17	−0.19	−0.17	−0.05
$\log g$, +0.1	$\Delta \log g$	−0.06	−0.07	−0.06	0.03
Photoionizations:					
Hydrogenic	Δ_{RBF}	−0.10	—	−0.16	—
Electron-impact ionizations:					
Rates $\times 10$	Δ_{CBF}	−0.05	−0.01	−0.09	<0.01
Electron-impact excitations:					
vReg, $\Upsilon = 1$	Δ_{CBB}	−0.01	—	0.01	—
	σ_{tot}	0.22	0.20	0.26	0.06
	σ_1	0.01	—	0.05	0.01
Average Δ_{NLTE}		0.51	0.38	−0.01	—

Sr; however, they are rather strong and the obtained $[\text{Sr}/\text{H}] = 0.38$ cannot be considered as a reliable value. Only Sr was measured in π Cet, and it has a normal (solar) abundance. No element beyond Fe was detected in the hottest star, ι Her.

In the following, we investigate whether the obtained enhancement of the neutron-capture (n-capture) elements in 21 Peg can be explained by errors of the abundance determinations or such a phenomenon is characteristic of A and late B-type stars with low rotational velocities.

5.1.1 Uncertainties in the NLTE abundances of heavy elements

We checked a sensitivity of the NLTE abundances from lines of Sr II, Zr II, Ba II, and Nd III in 21 Peg to variations in atmospheric parameters and atomic data used in the NLTE calculations. Table 5 summarizes results of our tests.

Fossati et al. (2009) estimate the uncertainties in T_{eff} , $\log g$, and ξ_i of 21 Peg as 200 K, 0.1 dex, and 0.5 km s^{−1}, respectively. Since enhancements of Sr and Zr are due to large positive NLTE abundance corrections, we have chosen to decrease T_{eff} , but increase $\log g$ in our test calculations. We do not indicate abundance shifts due to variations in ξ_i , because all the lines under investigation are weak, with EW < 30 mÅ.

We assumed that a maximal influence of variations in photoionization cross-sections on the NLTE results can be estimated when replacing accurate data from the DBSR method (see Section 3.2) with the hydrogenic cross-sections. Such estimates can be done for Sr II and Ba II. Since the NLTE effects were reduced, when using hydrogenic photoionization cross-sections, we assume that our calculations for Zr II provided the lower limit for the Zr NLTE abundance. Variations in photoionization cross-sections cannot affect the NLTE abundances derived from lines of Nd III because Nd III is a majority species in the atmosphere of 21 Peg.

For Sr II, Zr II, and Ba II, the main NLTE mechanism is the overionization. The NLTE effects can be reduced, by increasing the electron-impact ionization rates. We have chosen a scaling factor of 10.

For Sr II and Ba II, we also checked the changes in the derived NLTE abundances, when replacing accurate electron-impact excitation data from Bautista et al. (2002) for Sr II and from Crandall et al. (1974) and Sobelman et al. (1981) for Ba II with the formula of van Regemorter (1962) for all allowed transitions and $\Upsilon = 1$ for all forbidden transitions. The corresponding string in Table 5 is denoted as vReg, $\Upsilon = 1$.

It can be seen from Table 5 that, for Sr II and Ba II, a variation in photoionization cross-sections has the bigger effect on the departures from LTE compared with that for a variation in collisional data. The total impact of varying each of the four parameters, σ_{tot} , was computed as the quadratic sum of ΔT_{eff} , $\Delta \log g$, Δ_{RBF} , and Δ_{CBF} . For comparison, we indicate the abundance error that is characteristic of the line-to-line scatter, σ_1 , and the average Δ_{NLTE} . For none of the four chemical elements, their obtained enhancements cannot be explained by the uncertainties in abundance determinations. Barium and neodymium have substantially supersolar abundances, independent of whether LTE or NLTE abundances are determined.

5.1.2 Comparison with the literature

For each of the four stars, a vast number of abundance determinations were made in the literature, mostly under the LTE assumption; see, for example, Adelman (1998) for ι Her and Fossati et al. (2009, and references therein) for 21 Peg and π Cet. The NLTE abundances were derived for ι Her (Nieva & Przybilla 2012, C, N, O, Ne, Mg, Si, Fe) and a limited number of chemical elements (Na, K, Ca, Sr, Ba) in HD 32115 (Bikmaev et al. 2002). The latter paper is based on the NLTE methods, which are very similar to that applied in this study. Small differences in the NLTE abundances between the two studies are due to using different observed spectra of HD 32115. For common elements in ι Her, our NLTE results agree very well with that of NP12.

Element abundance pattern of π Cet, as obtained by Fossati et al. (2009, F09) under the LTE assumption, observed emission features at the position of the C I lines in the near-IR and close to the core of H α , and the variations in the line profiles within 1 d make doubt in a status of π Cet as a normal star. The NLTE calculations remove most of the problems of the LTE analysis and provide a firm evidence for π Cet being an abundance standard of a normal B-type star. Indeed, Alexeeva et al. (2016) showed that the emission in C I 8335 and 9405 Å appears due to the departures from LTE and these emission lines form in the atmosphere of π Cet. NLTE removes an overabundance of O, Ne, Na, and Mg and an underabundance of Ti obtained by F09.

Compared with detailed LTE abundances reported by F09 for 21 Peg, our NLTE calculations remove an overabundance of Ne and an underabundance of Ca relative to their solar abundances. Based on our NLTE calculations for Zr II, we expect positive NLTE abundance corrections for lines of Sc II, at the level of 0.5 dex (see Section 4.3). Solar abundances of Ca and Sc in 21 Peg are in particular important because subsolar Ca as well Sc abundances serve as formal classification criteria of Am stars. We, thus, exclude finally an assumption that 21 Peg could be the hottest known Am star. We also note that NLTE removes a big abundance discrepancy between Si II and Si I obtained by F09.

Inspecting the literature leads us to conclude that enhancement of the n-capture elements, as found for 21 Peg and HD 32115, is a widely spread phenomenon among chemically normal A-type stars (Lemke 1990; Hill & Landstreet 1993; Adelman 1998, and references therein). In Fig. 6, we compare our NLTE abundance patterns with the literature data for superficially normal stars. These are ι Her and 18 Peg from Nieva & Przybilla (2012, NLTE) and γ Gem from Adelman et al. (2015b, LTE). The stars ι Her and 18 Peg ($T_{\text{eff}} = 15\,800$ K) are too hot for reliable measurements of any of the n-capture elements in the visible spectra. The star γ Gem, with $T_{\text{eff}} = 9150$ K, is referred to as a classical superficially normal A-type star. In order to display element abundance pattern of γ Gem, we selected

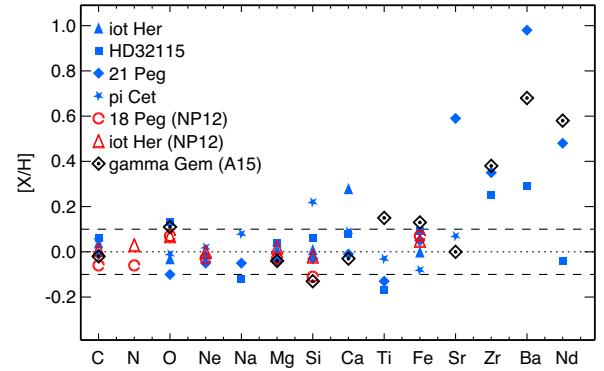


Figure 6. Element abundance patterns of the superficially normal stars. Our NLTE abundances for ι Her (filled triangles), HD 32115 (squares), 21 Peg (filled rhombi), and π Cet (five-pointed stars) compared with NLTE abundances of 18 Peg (circles) and ι Her (open triangles) from Nieva & Przybilla (2012, NP12) and LTE abundances of γ Gem (rhombi with a small circle inside) from Adelman, Gulliver & Kaewkornmaung (2015b, A15). The dashed lines indicate typical abundance error of 0.1 dex. Note that the hotter star the higher abundances of Zr, Ba, and Nd are.

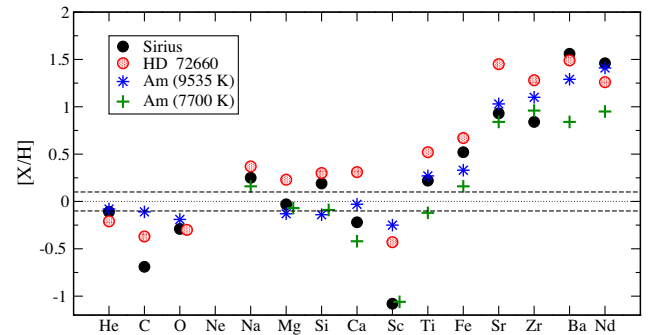


Figure 7. Element abundance patterns of the Am stars. Our sample stars Sirius and HD 72660 compared with σ Peg (Adelman, Gulliver & Heaton 2015a, $T_{\text{eff}} = 9535$ K) and 32 Aqr (Adelman et al. 1997, $T_{\text{eff}} = 7700$ K).

the abundances derived by Adelman et al. (2015b) from lines of C II, O I, Mg II, Si II, Ca I–II, Ti I, and Fe II, for which the NLTE abundance corrections are minor, according to our estimates. For Sr, Zr, and Ba, their NLTE abundances would be higher than the LTE ones, by 0.2–0.3 dex. It is evident that 21 Peg, γ Gem, and HD 32115 reveal an enhancement of the n-capture elements, and its magnitude correlates with T_{eff} . The hotter star, the higher abundances of the heavy elements are.

5.2 Am stars

Sirius and HD 72660 were previously classified as hot Am stars by Landstreet (2011, and references therein) and Varenne (1999), respectively. They have similar T_{eff} and $\log g$; however, HD 72660 has higher abundances of metals in the range from Na to Fe, by 0.1 dex (Si) to 0.5 dex (Ca). The NLTE abundances of Sirius and HD 72660 are compared in Fig. 7 with the LTE abundances of classical hot Am star σ Peg (Adelman et al. 2015a) and cool Am star 32 Aqr (Adelman et al. 1997). Both Am stars of our sample follow a general abundance trend of the Am stars. They have a deficit of Sc (the key element in Am classification) relative to nearby chemical elements, although of different magnitude for Sirius and HD 72660.

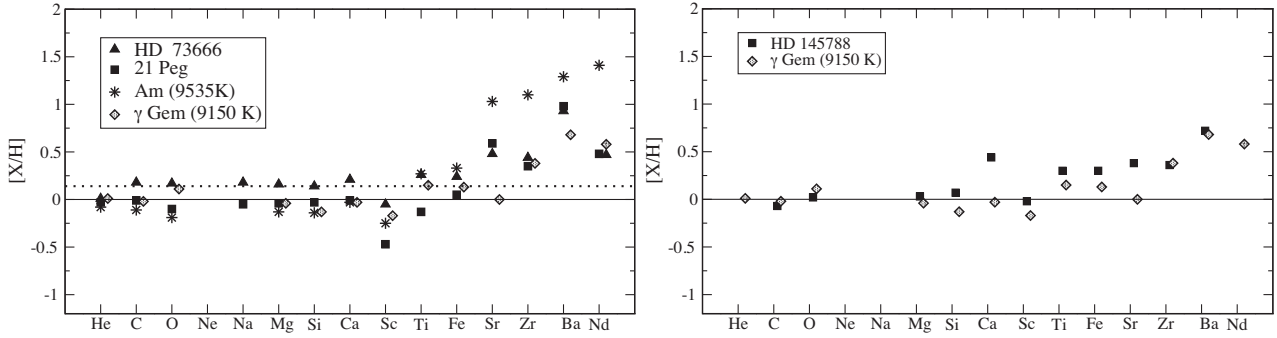


Figure 8. Element abundance patterns of HD 73666 (left-hand panel) and HD 145788 (right-hand panel) compared with that of an Am star *o* Peg (Adelman et al. 2015a, $T_{\text{eff}} = 9535$ K) and superficially normal stars 21 Peg (this work) and γ Gem (Adelman et al. 2015b). The dotted line indicates a metallicity of the Praesepe open cluster, $[\text{Fe}/\text{H}] = 0.14$ (Chen et al. 2003). See the text for a discussion of expected NLTE abundance corrections for Sc.

This does not make doubt in their status of Am stars, because *o* Peg and 32 Aqr also reveal rather different underabundances of Sc.

5.3 HD 73666

Based on their LTE abundance analysis, Fossati et al. (2007) refer to HD 73666 as a normal A-type star. We now look at this star from the NLTE perspective. Element abundance pattern of HD 73666 is displayed in Fig. 8 together with abundances of a classical hot Am star *o* Peg (Adelman et al. 2015a, LTE, $T_{\text{eff}} = 9535$ K) and two superficially normal stars: 21 Peg (this study, NLTE) and γ Gem (Adelman et al. 2015b, LTE, $T_{\text{eff}} = 9150$ K). Elements from C to Ca in HD 73666 reveal very similar overabundances of 0.14–0.20 dex relative to their solar abundances, in line with the cluster metallicity: $[\text{Fe}/\text{H}] = 0.14$ (Chen, Hou & Wang 2003) and 0.11 (Fossati et al. 2008). There is a hint of the higher enhancement for the heavier elements Ti and Fe, with $[\text{Ti}/\text{H}] = 0.26$ and $[\text{Fe}/\text{H}] = 0.24$. The LTE abundance of Sc reveals a deficit of $[\text{Sc}/\text{H}] = -0.05$. As discussed in Section 4.3, we expect the NLTE abundance corrections for lines of Sc II to be similar to that for Zr II. For HD 73666, the difference between NLTE and LTE abundances of Zr amounts to 0.19 dex, and we expect that NLTE would place Sc close to the other elements from C to Fe in the abundance pattern. We also expect that NLTE would largely remove deficit of Sc in 21 Peg, where $\Delta_{\text{NLTE}} = 0.51$ dex for Zr II 4149 Å. The comparison stars γ Gem and *o* Peg, most probably, do not have a deficit of Sc as well. Abundances of the heavy elements in HD 73666 agree with those for the superficially normal stars 21 Peg and γ Gem.

Compared with the LTE abundance analysis of Fossati et al. (2007), NLTE reduces overabundances of C, O, and Na to the level characteristic of the other elements and removes substantial abundance discrepancies between Mg I and Mg II and between Ca I and Ca II, increasing, thus, a credit of confidence in the obtained element abundance pattern. Our NLTE abundance analysis provides a firm evidence for HD 73666 being a chemically normal star despite catastrophic processes in the Praesepe open cluster that led to the formation of a Blue Straggler.

5.4 HD 145788

The star HD 145788 was studied by Fossati et al. (2009), who find an overall enhancement of metals, but do not find the Sc deficit that is a typical classification characteristic of an Am star. They come to the conclusion that, similarly to HD 73666, HD 145788 is a normal star reflecting a chemical composition of the cloud where

it formed. Fig. 8 shows the NLTE abundance pattern of this star in comparison with the LTE abundances of γ Gem (Adelman et al. 2015b). HD 145788 has close-to-solar abundances of C, O, Mg, and Si, while Ti and Fe are enhanced at the level of 0.3 dex. The higher overabundance was obtained for Ca, $[\text{Ca}/\text{H}] = 0.44$. Scandium can be slightly enhanced, if the NLTE effects for Sc II are similar to that for Zr II. Overabundances of the elements heavier than Fe are similar to that for the superficially normal star of similar temperature, γ Gem, but substantially lower compared with that for the Am stars of similar temperature, HD 72660 and Sirius.

The calculated overabundances of Ti to Ba cannot be caused by the NLTE treatments because LTE leads to even higher $[\text{X}/\text{H}]$ for Ti, Fe, and Sr and the same $[\text{Ba}/\text{H}]$ (Table 3). They cannot be due to underestimated microturbulent velocity. We used $\xi_t = 1.3 \text{ km s}^{-1}$, as derived by Fossati et al. (2009) and proved by Sitnova et al. (2016) in NLTE analysis of the Ti II lines. With our detailed NLTE analysis, we cannot clarify the status of HD 145788.

5.5 Superficially normal versus Am stars

Careful NLTE abundance study of eight slowly rotating A- and B-type stars shows that they have a common feature. This is overabundances of the n-capture elements Sr, Zr, Ba, and Nd, although they are observed at different levels in superficially normal and Am stars. The question arises: how the observed overabundances of heavy elements in A stars are connected with stellar characteristics, such as rotation, magnetic field, binarity, effective temperature?

Royer et al. (2014) show that the LTE abundances of Y, Zr, and Ba in 21 normal A1–A2 ($T_{\text{eff}} > 8900$ K) stars are supersolar, with the median values $[\text{Y}/\text{H}] \simeq 0.15$, $[\text{Zr}/\text{H}] \simeq 0.5$, and $[\text{Ba}/\text{H}] \simeq 0.8$. In this temperature range, our NLTE calculations predict positive NLTE abundance corrections for lines of Zr II and Ba II. This means an even greater discrepancy with the solar abundances. Strontium is probably also supersolar, because Royer et al. (2014) obtain $[\text{Sr}/\text{H}] \simeq -0.25$ in LTE, while the NLTE abundance corrections can be at the level of +0.5 dex for lines of Sr II. It is interesting that the comparison sample composed of nine normal A-type stars from the Pleiades and the Ursa Major moving group has the LTE abundances close, on average, to solar abundances of Y–Ba. Royer et al. (2014) note that different rotation velocities can be a source of discrepancies between the two stellar samples because the main sample stars have $v \sin i \leq 65 \text{ km s}^{-1}$, while seven of nine comparison stars have $100 \leq v \sin i \leq 200 \text{ km s}^{-1}$.

Fossati et al. (2008) search for abundance trends with respect to T_{eff} and $v \sin i$ for three samples of the Am and A- and F-type stars in the Praesepe cluster. All their stars are cooler than 8200 K. This

can explain the lower enhancement of Ba, at the level of 0.5 dex, in the normal A-type stars compared with the corresponding value reported by Royer et al. (2014). The normal A and Am stars have different $v \sin i$, with A-type stars being faster rotators ($v \sin i = 75\text{--}190 \text{ km s}^{-1}$) compared with the Am stars ($v \sin i \leq 70 \text{ km s}^{-1}$). The Am stars reveal high abundances of heavy elements, with [Y/H] and [Ba/H] of up to 1.2 and 2 dex, respectively, which decrease with $v \sin i$ and approach the corresponding abundances of the slowest rotators among the normal A-type stars. No clear correlation is found between abundance and T_{eff} and between abundance and $v \sin i$ for the normal A-type stars. The former can be due to missing the $T_{\text{eff}} > 8500 \text{ K}$ stars.

Varenne & Monier (1999) make similar analysis for the Hyades open cluster. Their sample of the normal A and Am stars covers similar T_{eff} range, with the only star of $T_{\text{eff}} > 8300 \text{ K}$, and similar $v \sin i$ range, with the only star of $v \sin i > 200 \text{ km s}^{-1}$. Fig. 8 in Varenne & Monier (1999) shows a hint of correlation between Ba abundance and $v \sin i$, although, in each of three $v \sin i$ ranges, that is $v \sin i \leq 50 \text{ km s}^{-1}$, $50 < v \sin i \leq 100 \text{ km s}^{-1}$, and $v \sin i > 100 \text{ km s}^{-1}$, the statistics of stars is poor and a scatter of [Ba/H] exceeds 0.5 dex.

The Am star Sirius possesses an ultra-weak global magnetic field ($< 1 \text{ G}$; Petit et al. 2011), while no information about magnetic field of HD 72660 is known. Recently, Blazère et al. (2020) measured a 10 G averaged magnetic field in a superficially normal A star γ Gem. Based on some common characteristics of γ Gem and Sirius (presence of the magnetic field and belonging to binary systems) and despite their rather different atmospheric chemistry, the authors classify γ Gem as a definite/potential Am star. Global magnetic field and the SrNd overabundances are characteristics of Ap stars, but it is unlikely that the same mechanism produces overabundances of heavy elements in Am and Ap stars. In contrast to the Am stars, where all the elements beyond Sr are overabundant by approximately the same amount, the Ap stars reveal enhancements of Sr and REE's at the level of 2–3 dex, while normal or moderately overabundant Zr and Ba (see fig. 2 in Romanovskaya et al. 2019).

We note that no large-scale magnetic field at the level of a few gauss was detected in 21 Peg (Kochukhov et al. 2013) and HD 73666 (Fossati et al. 2007), which reveal substantial enhancements of heavy elements.

Peculiar abundances of the n-capture elements in the atmospheres of superficially normal slowly rotating stars are produced, probably, by the same mechanism as that responsible for the Am phenomenon. However, it operates less efficiently, resulting in only moderate enhancements of the n-capture elements and close-to-solar abundances of Fe and the lighter elements. The question is whether the Am phenomenon is a manifestation of a certain stage of the star's evolution. Can superficially normal A and late B stars with low rotational velocities be nascent Am stars? Or on the contrary, did they already pass the Am stage? Or is there no relationship between normal A and Am stars?

We note that, in HD 32115 and 21 Peg, barium has greater overabundance relative to the solar value compared with that for the other heavy elements. The published abundances of heavy elements in young ($< 2 \text{ Gyr}$) open clusters and associations (D'Orazi et al. 2009; Jacobson & Friel 2013; Mishenina et al. 2015; Overbeek et al. 2015; Reddy & Lambert 2015; D'Orazi, De Silva & Melo 2017) find a statistically significant trend of increasing cluster [Ba/Fe] as a function of decreasing cluster age, while all the other n-capture elements, such as Y, Zr, La, and Ce, exhibit a solar-scaled pattern. Various ideas were suggested to explain extra production of Ba, for example, enhanced s-process production in low-mass ($1\text{--}1.5 M_{\odot}$) AGB stars with highly effective mixing (D'Orazi et al. 2009) or the intermediate neutron-capture process (Mishenina et al. 2015);

however, the origin of extra amount of Ba in young stellar systems remains the puzzle. Could it be that the solar value does not represent the modern galactic abundance of Ba and our sample stars, which all are less than 1 Gyr old, formed from the matter enriched with Ba more than the Sun?

5.6 Vega

Venn & Lambert (1990) identified Vega as a mild λ Bootis star. As shown first by Baschek & Slettebak (1988), these types of stars have essentially normal (solar) abundances of the light elements (C, N, and O) and the underabundances of the heavier elements (Mg, Al, Si, S, Mn, Fe, and Ni). Abundance anomalies are associated with the accretion of metal-poor material from a circumstellar disc or cloud (Venn & Lambert 1990).

Compared with published NLTE abundances of Vega, this study supplemented its NLTE abundance pattern by Si, Ca, Ti, and Zr. We obtained only slightly subsolar abundances of C ([C/H] = -0.05) and O ([O/H] = -0.13) and deficit of Mg, Si, Ca, Ti, and Fe, with [X/H] of -0.3 down to -0.6 dex. These results are in line with a status of Vega as a mild λ Bootis star. Heavy elements Sr, Zr, and Ba turn out to be less underabundant, with [X/H] between -0.19 and -0.04 .

For common chemical elements (C, O, Mg, Fe, Sr, and Ba), our NLTE abundances agree within 0.01–0.10 dex with the earlier determinations of Gigas (1986, 1988), Sturenburg & Holweger (1991), Takeda (1992), Belyakova et al. (1999), and Przybilla et al. (2000, 2001a, b).

6 CONCLUSIONS

This study presents a comparative analysis of the element abundance patterns of the stellar sample that includes slowly rotating superficially normal, Am, λ Bootis-type stars and the two stars with unidentified type of chemical peculiarity. The abundance patterns include 14 chemical elements in the range from He to Nd. In order to increase a confidence in our results and conclusions, we use the stars with well-determined atmospheric parameters and high-quality observed spectra available and derive chemical abundances based on the NLTE line formation. The NLTE methods for He I, C I, O I, Ne I, Mg I–II, Si I–II–III, Ca I–II, and Ti I–II were treated in our earlier studies. Here, we present first determinations of the NLTE abundances for Na, Sr, Zr, Ba, and Nd in the sample stars. The exception is Vega, for which the NLTE abundances of Sr and Ba were derived earlier by Belyakova et al. (1999) and Gigas (1988), respectively.

We constructed new model atom of Zr II–III and showed that, in the stellar parameter range with which we concern, NLTE leads to weakened lines of Zr II, with positive NLTE abundance corrections of 0.05 up 0.5 dex depending on T_{eff} , while strengthened lines of Zr III, with negative NLTE abundance corrections at the level of $(-0.1)\text{--}(-0.2)$ dex. For HD 72660, we obtained consistent NLTE abundances from lines of the two ionization stages, Zr II and Zr III, while the difference in LTE abundances amounts to -0.28 dex.

The NLTE calculations for Sr II and Ba II were performed using for the first time accurate photoionization cross-sections, which were calculated for this study with the Dirac *B*-spline *R*-matrix (DBSR) method, in the same approximations as Zatsarinny & Tayal (2010) adopted. In the hot ($T_{\text{eff}} > 9000 \text{ K}$) atmospheres, both Sr II and Ba II are subject to strong overionization resulting in weakened lines and positive NLTE abundance corrections. Depending on T_{eff} , they amount to 0.35–0.59 dex for Sr II 4077, 4215 Å and 0.26–0.38 dex for Ba II 4554, 4934 Å.

We obtained that the NLTE abundances of He to Fe in HD 32115 (He was not measured), 21 Peg, π Cet, and ι Her are consistent with the solar abundances of Lodders et al. (2009), mostly within 0.1 dex, providing a firm evidence for a status of these stars as superficially normal stars. We note that, for ι Her, our results support the earlier conclusion of Nieva & Przybilla (2012). Elements beyond the Fe group reveal pronounced enhancements in 21 Peg, at the level of 0.6, 0.35, and 0.5 dex for Sr, Zr, and Nd, respectively. Even larger deviation from the solar abundance, of one order of magnitude, was obtained for Ba. Strontium, zirconium, and barium are also enhanced in HD 32115, but to a less extent. Combining our results with the literature data on an enhancement of the n-capture elements in A-type stars, we conclude that its magnitude correlates with T_{eff} : The hotter star, the higher abundances of the heavy elements are. Only Sr of the n-capture elements was measured for π Cet, with the NLTE abundance close to the solar one. This star can be referred to as an abundance standard of a normal late B-type star.

In HD 73666 (a member of the Praesepe open cluster, a Blue Straggler), elements from C to Fe reveal an enhancement, which is close to the cluster metallicity: $[\text{Fe}/\text{H}] = 0.14$ dex (Chen et al. 2003) and 0.11 (Fossati et al. 2008). Heavy elements Sr, Zr, Ba, and Nd are overabundant, at the level similar to that for the superficially normal A-type stars of close temperature. Our NLTE abundance analysis provides a firm evidence for HD 73666 being a chemically normal star despite catastrophic processes that led to the formation of a Blue Straggler.

Although both Am stars of our sample, Sirius and HD 72660, have similar atmospheric parameters, they differ in chemical abundances. Generally, HD 72660 is more metal rich than Sirius except Ba and Nd that are slightly more abundant in Sirius. The enhancement of Sr, Zr, Ba, and Nd reaches 1.5 dex.

With our detailed NLTE analysis, we cannot clarify a status of HD 145788. This star has close-to-solar abundances of C, O, Mg, and Si, while Ca, Ti, and Fe are enhanced, at the level of 0.4–0.3 dex. In the range of heavy elements, beyond Sr, abundance pattern of HD 145788 resembles that for superficially normal A-type stars.

We propose that the same mechanism produces enhancements of the n-capture elements in the atmospheres of Am and superficially normal stars with low rotational velocities. However, in the latter type of objects, it operates less efficiently, not affecting abundances of Fe and the lighter elements and resulting in only moderate enhancements of heavy elements. To understand this mechanism(s) is a challenge for the physics of stars. Observations show that the level of enhancement of heavy elements is higher for the hotter stars and, probably, does not depend on the presence or absence of magnetic field.

Compared with the literature data, the NLTE abundance pattern of Vega was supplemented by Si, Ca, Ti, and Zr. In line with a status of Vega as a mild λ Bootis star, C and O have close-to-solar abundances and Mg to Fe are underabundant, at the level of 0.4 dex. Less underabundances, of (-0.19) – (-0.04) dex, were found for the heavy elements Sr, Zr, and Ba.

In every of our star with Ba abundance available, $[\text{Ba}/\text{H}]$ was found to be larger than $[\text{X}/\text{H}]$ for any other element X. Taking also into account published Ba abundances of young open clusters, we propose that the solar Ba abundance is not representative of the galactic Ba abundance at modern epoch.

ACKNOWLEDGEMENTS

The authors thank V. Khalack, A. J. Korn, and J. Landstreet for providing observed spectra of HD 72660 and Vega. LM, TR, and TS thank the Ministry of Science and Higher Education of Russian Federation (project 13.1902.21.0039) for a support of this study. This

study made use of the NIST, VALD, Astrophysics Data System,⁶ and R. Kurucz's data bases. The authors thank the referee Luca Fossati for his constructive suggestions and remarks.

DATA AVAILABILITY

The data underlying this article will be shared on reasonable request to the corresponding author.

REFERENCES

- Adelman S. J., 1998, *MNRAS*, 296, 856
 Adelman S. J., Caliskan H., Kocer D., Bolcal C., 1997, *MNRAS*, 288, 470
 Adelman S. J., Caliskan H., Kocer D., Cay I. H., Gokmen Tektunali H., 2000, *MNRAS*, 316, 514
 Adelman S. J., Gulliver A. F., Heaton R. J., 2015a, *PASP*, 127, 58
 Adelman S. J., Gulliver A. F., Kaewkornmaung P., 2015b, *PASP*, 127, 340
 Alexeeva S., Pakhomov Y., Mashonkina L., 2014, *Astron. Lett.*, 40, 406
 Alexeeva S. A., Ryabchikova T. A., Mashonkina L. I., 2016, *MNRAS*, 462, 1123
 Alexeeva S., Ryabchikova T., Mashonkina L., Hu S., 2018, *ApJ*, 866, 153
 Alexeeva S., Chen T., Ryabchikova T., Shi W., Sadakane K., Nishimura M., Zhao G., 2020, *ApJ*, 896, 59
 Barklem P. S., Piskunov N., O'Mara B. J., 2000, *A&AS*, 142, 467
 Baschek B., Slettebak A., 1988, *A&A*, 207, 112
 Bautista M. A., Gull T. R., Ishibashi K., Hartman H., Davidson K., 2002, *MNRAS*, 331, 875
 Belyakova E. V., Mashonkina L. I., 1997, *Astron. Rep.*, 41, 530
 Belyakova E. V., Mashonkina L. I., Sakhibullin N. A., 1999, *Astron. Rep.*, 43, 819
 Bikmaev I. F. et al., 2002, *A&A*, 389, 537
 Blazère A., Petit P., Neiner C., Folsom C., Kochukhov O., Mathis S., Deal M., Landstreet J., 2020, *MNRAS*, 492, 5794
 Borghs G., de Bisschop P., van Hove M., Silverans R. E., 1983, *Hyperfine Interact.*, 15, 177
 Bruls J. H. M. J., Rutten R. J., Shchukina N. G., 1992, *A&A*, 265, 237
 Butler K., Giddings J., 1985, Newsletter on the Analysis of Astronomical Spectra, No. 9. Univ. London, London, UK
 Castelli F., Kurucz R. L., 1993, in Dworetsky M. M., Castelli F., Faraggiana R., eds, ASP Conf. Ser. Vol. 44, IAU Colloq. 138: Peculiar Versus Normal Phenomena in A-Type and Related Stars. Astron. Soc. Pac., San Francisco, p. 496
 Chen L., Hou J. L., Wang J. J., 2003, *AJ*, 125, 1397
 Cowley C. R., 1971, *The Observatory*, 91, 139
 Crandall D. H., Taylor P. O., Dunn G. H., 1974, *Phys. Rev. A*, 10, 141
 D'Orazi V., Magrini L., Randich S., Galli D., Busso M., Sestito P., 2009, *ApJ*, 693, L31
 D'Orazi V., De Silva G. M., Melo C. F. H., 2017, *A&A*, 598, A86
 De Munshi D., Dutta T., Rebhi R., Mukherjee M., 2015, *Phys. Rev. A*, 91, 040501
 Dutta T., de Munshi D., Yum D., Rebhi R., Mukherjee M., 2016, *Sci. Rep.*, 6, 29772
 Fossati L., Bagnulo S., Monier R., Khan S. A., Kochukhov O., Landstreet J., Wade G., Weiss W., 2007, *A&A*, 476, 911
 Fossati L., Bagnulo S., Landstreet J., Wade G., Kochukhov O., Monier R., Weiss W., Gebran M., 2008, *A&A*, 483, 891
 Fossati L., Ryabchikova T., Bagnulo S., Alecian E., Grunhut J., Kochukhov O., Wade G., 2009, *A&A*, 503, 945 (F09)
 Fossati L., Mochnacki S., Landstreet J., Weiss W., 2010, *A&A*, 510, A8
 Gigas D., 1986, *A&A*, 165, 170
 Gigas D., 1988, *A&A*, 192, 264
 Golriz S. S., Landstreet J. D., 2016, *MNRAS*, 456, 3318
 Henderson M., Irving R. E., Matulioniene R., Curtis L. J., Ellis D. G., Wahlgren G. M., Brage T., 1999, *ApJ*, 520, 805

⁶http://adsabs.harvard.edu/abstract_service.html

- Hill G. M., Landstreet J. D., 1993, *A&A*, 276, 142
- Jacobson H. R., Friel E. D., 2013, *AJ*, 145, 107
- Khokhlova V. L., Ryabchikova T. A., 1975, *Ap&SS*, 34, 403
- Kochukhov O. et al., 2013, *A&A*, 554, A61
- Korotin S. A., Ryabchikova T. A., 2018, *Astron. Lett.*, 44, 621
- Kramida A., Ralchenko Y., Reader J., NIST ASD Team, 2019, NIST Atomic Spectra Database (Version 5.7.1). Available at: <http://physics.nist.gov/asd>
- Landstreet J. D., 2011, *A&A*, 528, A132
- Lawler J. E., Dakin J. T., 1989, *J. Opt. Soc. Am. B*, 6, 1457
- Lemke M., 1990, *A&A*, 240, 331
- Ljung G., Nilsson H., Asplund M., Johansson S., 2006, *A&A*, 456, 1181
- Lodders K., Plame H., Gail H.-P., 2009, in Trümper J. E., ed., *Landolt-Börnstein – Group VI Astronomy and Astrophysics Numerical Data and Functional Relationships in Science and Technology Volume 4B: Solar System*. Springer-Verlag, Berlin, p. 44
- Lyubimkov L. S., Lambert D. L., Korotin S. A., Poklad D. B., Rachkovskaya T. M., Rostopchin S. I., 2011, *MNRAS*, 410, 1774
- Lyubimkov L. S., Lambert D. L., Korotin S. A., Rachkovskaya T. M., Poklad D. B., 2015, *MNRAS*, 446, 3447
- Lyubimkov L. S., Korotin S. A., Lambert D. L., 2019, *MNRAS*, 489, 1533
- McWilliam A., 1998, *AJ*, 115, 1640
- Mansour N. B., Dinneen T., Young L., Cheng K. T., 1989, *Phys. Rev. A*, 39, 5762
- Mashonkina L., 2020, *MNRAS*, 493, 6095
- Mashonkina L., Gehren T., Bikmaev I., 1999, *A&A*, 343, 519
- Mashonkina L., Ryabchikova T., Ryabtsev A., 2005, *A&A*, 441, 309
- Mayo R., Ortiz M., Campos J., 2005, *J. Quant. Spectrosc. Radiat. Transfer*, 94, 109
- Michaud G., 1970, *ApJ*, 160, 641
- Michaud G., 1980, *AJ*, 85, 589
- Michaud G., 1982, *ApJ*, 258, 349
- Mishenina T. et al., 2015, *MNRAS*, 446, 3651
- Nieva M.-F., Przybilla N., 2012, *A&A*, 539, A143 (NP12)
- Overbeek J. C., Friel E. D., Jacobson H. R., Johnson C. I., Pilachowski C. A., Mészáros S., 2015, *AJ*, 149, 15
- Pakhomov Y. V., Ryabchikova T. A., Piskunov N. E., 2019, *Astron. Rep.*, 63, 1010
- Petit P. et al., 2011, *A&A*, 532, L13
- Preston G. W., 1974, *ARA&A*, 12, 257
- Przybilla N., Butler K., 2001, *A&A*, 379, 955
- Przybilla N., Butler K., Becker S. R., Kudritzki R. P., Venn K. A., 2000, *A&A*, 359, 1085
- Przybilla N., Butler K., Becker S. R., Kudritzki R. P., 2001a, *A&A*, 369, 1009
- Przybilla N., Butler K., Kudritzki R. P., 2001b, *A&A*, 379, 936
- Przybilla N., Butler K., Becker S. R., Kudritzki R. P., 2006, *A&A*, 445, 1099
- Przybilla N., Nieva M. F., Tillich A., Heber U., Butler K., Brown W. R., 2008, *A&A*, 488, L51
- Przybilla N., Nieva M.-F., Butler K., 2011, *J. Phys. Conf. Ser.*, 328, 012015
- Przybilla N., Aschenbrenner P., Buder S., 2017, *A&A*, 604, L9
- Reader J., Acquista N., 1997, *Phys. Scr.*, 55, 310
- Reddy A. B. S., Lambert D. L., 2015, *MNRAS*, 454, 1976
- Romanovskaya A., Ryabchikova T., Shulyak D., Perraut K., Valyavin G., Burlakova T., Galazutdinov G., 2019, *MNRAS*, 488, 2343
- Royer F. et al., 2014, *A&A*, 562, A84
- Ryabchikova T., Piskunov N., Kurucz R. L., Stempels H. C., Heiter U., Pakhomov Y., Barklem P. S., 2015, *Phys. Scr.*, 90, 054005
- Rynkun P., Gaigalas G., Jönsson P., 2020, *A&A*, 637, A10
- Sadakane K., 1981, *PASP*, 93, 587
- Schiller F., Przybilla N., 2008, *A&A*, 479, 849
- Seaton M. J., 1962, in Bates D. R., ed., *Atomic and Molecular Processes*. Academic Press, New York, p. 375
- Shulyak D., Tsymbal V., Ryabchikova T., Stütz C., Weiss W. W., 2004, *A&A*, 428, 993
- Sitnova T. M., Mashonkina L. I., Ryabchikova T. A., 2013, *Astron. Lett.*, 39, 126
- Sitnova T. M., Mashonkina L. I., Ryabchikova T. A., 2016, *MNRAS*, 461, 1000
- Sitnova T. M., Mashonkina L. I., Ryabchikova T. A., 2018, *MNRAS*, 477, 3343
- Sobelman I. I., Vainshtein L. A., Yukov E. A., 1981, *Excitation of Atoms and Broadening of Spectral Lines*. Springer Series Chem. Phys. 7. Springer, Berlin
- Steenbock W., Holweger H., 1992, in Heber U., Jeffery C. S., eds, *Statistical Equilibrium of Al I/II in a Stars and the Abundance of Aluminium in Vega*. Springer-Verlag, Berlin, p. 57
- Sturenburg S., Holweger H., 1991, *A&A*, 246, 644
- Takeda Y., 1992, *PASJ*, 44, 649
- Takeda Y., Takada-Hidai M., 2000, *PASJ*, 52, 113
- Takeda Y., Kawanomoto S., Ohishi N., 2007, *PASJ*, 59, 245
- Takeda Y., Kang D.-I., Han I., Lee B.-C., Kim K.-M., 2009, *PASJ*, 61, 1165
- Tsymbal V., Ryabchikova T., Sitnova T., 2019, in Kudryavtsev D. O., Romanyuk I. I., Yakunin I. A., eds, *ASP Conf. Ser. Vol. 518, Physics of Magnetic Stars*. Astron. Soc. Pac., San Francisco, p. 247
- Unsold A., 1955, *Physik der Sternatmosphären*, MIT Besonderer Berücksichtigung der Sonne. Springer, Berlin
- van Regemorter H., 1962, *ApJ*, 136, 906
- Varenne O., 1999, *A&A*, 341, 233
- Varenne O., Monier R., 1999, *A&A*, 351, 247
- Velichko A. B., Mashonkina L. I., Nilsson H., 2010, *Astron. Lett.*, 36, 664
- Venn K. A., 1995, *ApJ*, 449, 839
- Venn K. A., Lambert D. L., 1990, *ApJ*, 363, 234
- Villemoes P., van Leeuwen R., Arnesen A., Heijlskjöld F., Kastberg A., Larsson M. O., Kotochigova S. A., 1992, *Phys. Rev. A*, 45, 6241
- Zatsarinny O., Tayal S. S., 2010, *Phys. Rev. A*, 81, 043423
- Zhang H. W., Gehren T., Zhao G., 2008, *A&A*, 481, 489
- Zhao G. et al., 2016, *ApJ*, 833, 225

SUPPORTING INFORMATION

Supplementary data are available at *MNRAS* online.

table2.dat

Please note: Oxford University Press is not responsible for the content or functionality of any supporting materials supplied by the authors. Any queries (other than missing material) should be directed to the corresponding author for the article.

This paper has been typeset from a \LaTeX file prepared by the author.